

Edinburgh 96/22  
 DFTT 58/96  
 hep-ph/9609515

## Measurement of the Polarized Structure Function $g_1^p(x, Q^2)$ at HERA

R. D. Ball<sup>a</sup>, A. Deshpande<sup>b,1</sup>, S. Forte<sup>c</sup>, V. W. Hughes<sup>b,2</sup>, J. Lichtenstadt<sup>d,e,3</sup>, G. Ridolfi<sup>f</sup>

Department of Physics and Astronomy, Edinburgh EH9 3JZ, Scotland<sup>(a)</sup>

Department of Physics, Yale University, New Haven, CT 06511, USA<sup>(b)</sup>

INFN, Sezione di Torino, I-10125 Torino, Italy<sup>(c)</sup>

CERN, CH-1211 Geneva 23, Switzerland<sup>(d)</sup>

School of Physics and Astronomy, The Raymond and Beverly Sackler Faculty of Exact  
 Sciences, Tel Aviv University, Tel Aviv 69978, Israel<sup>(e)</sup>

INFN, Sezione di Genova, I-16146, Genova, Italy<sup>(f)</sup>

### Abstract

We present estimates of possible data on spin-dependent asymmetries in inclusive scattering of high energy polarized electrons by high energy polarized protons at HERA, including statistical errors, and discuss systematic uncertainties. We show that these data would shed light on the small  $x$  behaviour of the polarized structure function  $g_1$ , and would reduce substantially the uncertainty on the determination of the polarized gluon distribution.

Presented at the 1996 HERA Workshop  
 “Future Physics at HERA”

*To be published in the proceedings*

September 1996

---

<sup>1</sup>Royal Society University Research Fellow.

<sup>2</sup>Supported by the Department of Energy.

<sup>3</sup>Supported by the Israel Science Foundation of the Israeli Academy of Sciences.

# 1 Introduction

Nucleon structure, particularly as defined by its structure functions determined from lepton-nucleon inclusive electromagnetic scattering, is of fundamental importance and has provided crucial information for the development of perturbative QCD. The history of such experiments over the past forty years has shown that important new information has been obtained when measurements were extended to new kinematic regions. In the mid-1950's at Stanford, Hofstadter [1] extended measurements of elastic electron-proton scattering to a higher  $Q^2$  range of 1 (GeV/c)<sup>2</sup> and first observed that the proton has a finite size. In the late 1960's at SLAC Friedman, Kendall and Taylor [2] extended measurements of inelastic inclusive electron scattering to the deep inelastic region of  $Q^2 > 1$  (GeV/c)<sup>2</sup> and discovered the parton substructure of the proton.

The subfield of polarized lepton-proton scattering was initiated with the Yale-SLAC E80 and E130 experiments [3] which measured the spin-dependent structure function of the proton in the mid-1980's. These experiments were then followed up at CERN by the EM Collaboration which extended the kinematic range of the original measurements at SLAC to lower the  $x$  range from  $x = 0.1$  to 0.01 [4]. These data allowed a determination of the singlet component of the first moment of  $g_1$ , which in the naive parton model is the fraction of the proton spin carried by quarks: this was found to be compatible with zero, thereby violating the parton model Ellis-Jaffe sum rule at the three standard deviation level. This surprising result has stimulated a large amount of experimental and theoretical work on polarized structure functions [5]. New measurements of the spin dependent structure functions of the proton and the deuteron were made by the SM collaboration [6] at CERN and by E143 [7] at SLAC which extended the kinematic range to lower  $x$  and also reduced the statistical and systematic uncertainties significantly. Figure 1 shows all published measurements of the structure function  $g_1^p$ . These measurements, along with those made for the deuteron, allowed a better determination of the first moment of the spin structure functions and a verification of the Bjorken sum rule. Furthermore, they made a next-to leading order QCD analysis of the  $x$  and  $Q^2$  dependence of  $g_1$  possible, thereby allowing a determination of the first moment of the polarized gluon distribution [8].

In view of all this, it is important to consider in detail what measurements and accuracies may be obtained at HERA. The primary goal and motivation of HERA is to extend the kinematic range of electron-proton scattering. Thus far HERA research and its discoveries were the result of the new and vastly extended kinematic range in  $x$  and  $Q^2$ , both by a factor of about 100, provided by the collider [9, 10]. At present the 800 GeV proton beam at HERA is unpolarized (although the 25 GeV electron/positron beam has a natural polarization). If the proton beam were to be polarized, it would be possible to measure polarization asymmetries and thus explore spin dependent structure functions along with the spin-independent structure functions in the HERA kinematic range. In this paper we discuss what might be achieved from such a programme. We show that the data HERA could provide are clearly unique and cannot be obtained by present day experiments.

In section 2 we estimate the data that could be obtained, including the statistical errors, from inclusive polarized e-p scattering with HERA in the collider mode. We also discuss systematic errors and argue that they can be controlled within adequate limits. In section 3 we briefly review the relation of the structure function  $g_1$  to polarized parton distributions and the perturbative evolution equations satisfied by the latter, and summarize the status of polarized parton distributions extracted from presently available fixed target data. In section 4 we show

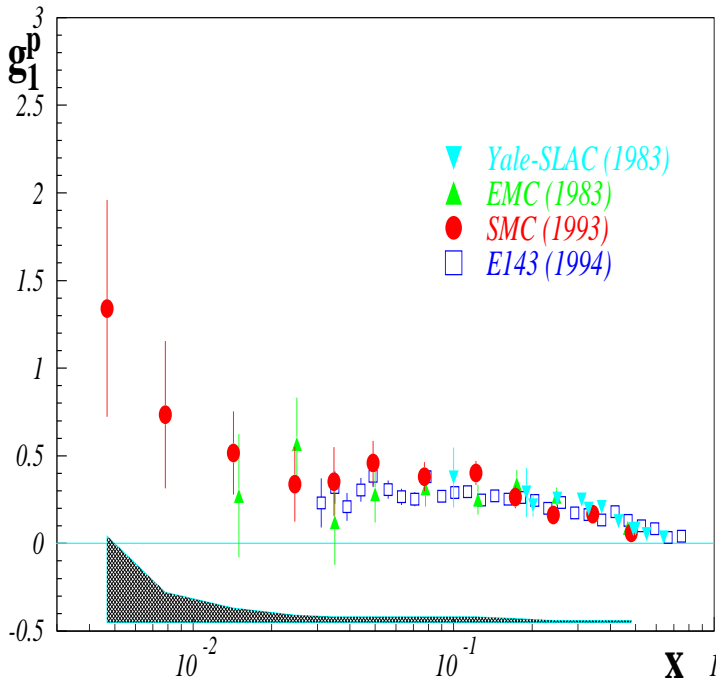


Figure 1: *The current status of the measurement of the spin structure function  $g_1^p$ . The statistical errors are shown with the data points, while the size of the systematic errors for the SMC measurement is shown by the shaded area.*

that new data from polarized colliding beam experiments at HERA would shed light on the small  $x$  behaviour of  $g_1$  and would substantially improve the determination of the polarized gluon distribution.

## 2 Measurement of $g_1^p(x, Q^2)$ at HERA

### 2.1 Kinematic range and statistical errors for HERA data

Presently all measurements of polarized structure functions are made using fixed target deep inelastic lepton-nucleon scattering. Figure 2 shows the kinematic ranges in which polarized lepton-proton data have been obtained at SLAC and CERN as well as the possible measurements in the kinematic domain available at HERA with 800 and 25 GeV proton and electron beams, respectively. Note the large extension in  $x - Q^2$  range compared to the present data. Table 1 lists the  $x - Q^2$  values at which measurements can be made at HERA, the number of events that would be measured and the associated statistical errors in the measured asymmetry  $\delta A_m$  assuming an integrated luminosity of  $L = 1000 \text{ pb}^{-1}$  and electron and proton polarizations of 0.7 each<sup>1</sup>. Kinematic cuts [9] on  $y$  and the scattered electron angle  $\theta'_e$  used for data analysis by the H1 and ZEUS collaborations were applied for the evaluation of the counting rates in each  $x - Q^2$  bin. Standard deep inelastic scattering formulae were used to calculate of the kinematics and asymmetries. They are given in the Appendix.

<sup>1</sup>Accelerator parameters that were suggested by R. Klanner and F. Willeke for this workshop.

$x$	$Q^2$ GeV <sup>2</sup>	$y$	$D$	$N_{total}$	$\delta A_m$
$5.6 \times 10^{-5}$	1.8	0.40	0.47	$5.0 \times 10^6$	$4.5 \times 10^{-4}$
$1.8 \times 10^{-4}$	1.8	0.13	0.13	$8.0 \times 10^6$	$3.5 \times 10^{-4}$
	5.6	0.40	0.46	$3.5 \times 10^6$	$5.3 \times 10^{-4}$
$5.6 \times 10^{-4}$	1.8	0.04	0.04	$1.2 \times 10^7$	$2.9 \times 10^{-4}$
	5.6	0.13	0.13	$6.5 \times 10^6$	$3.9 \times 10^{-4}$
	$1.8 \times 10^1$	0.40	0.47	$2.0 \times 10^6$	$7.1 \times 10^{-4}$
$1.8 \times 10^{-3}$	1.8	0.01	0.01	$1.6 \times 10^7$	$2.5 \times 10^{-4}$
	5.6	0.04	0.04	$9.0 \times 10^6$	$3.3 \times 10^{-4}$
	$1.8 \times 10^1$	0.13	0.13	$3.4 \times 10^6$	$5.4 \times 10^{-4}$
	$5.6 \times 10^1$	0.40	0.47	$1.1 \times 10^6$	$9.5 \times 10^{-4}$
$5.6 \times 10^{-3}$	5.6	0.01	0.01	$1.2 \times 10^7$	$2.8 \times 10^{-4}$
	$1.8 \times 10^1$	0.04	0.04	$5.5 \times 10^6$	$4.3 \times 10^{-4}$
	$5.6 \times 10^1$	0.13	0.13	$1.7 \times 10^6$	$7.7 \times 10^{-4}$
	$1.8 \times 10^2$	0.40	0.47	$5.5 \times 10^5$	$1.3 \times 10^{-3}$
$1.8 \times 10^{-2}$	$1.8 \times 10^1$	0.01	0.01	$6.5 \times 10^6$	$3.9 \times 10^{-4}$
	$5.6 \times 10^1$	0.04	0.04	$2.6 \times 10^6$	$6.2 \times 10^{-4}$
	$1.8 \times 10^2$	0.12	0.13	$8.0 \times 10^5$	$1.1 \times 10^{-3}$
	$5.6 \times 10^2$	0.40	0.47	$2.3 \times 10^5$	$2.1 \times 10^{-3}$
$5.6 \times 10^{-2}$	$5.6 \times 10^1$	0.01	0.01	$2.2 \times 10^6$	$6.7 \times 10^{-4}$
	$1.8 \times 10^2$	0.04	0.04	$8.0 \times 10^5$	$1.1 \times 10^{-3}$
	$5.6 \times 10^2$	0.12	0.13	$2.6 \times 10^5$	$2.0 \times 10^{-3}$
	$1.8 \times 10^3$	0.40	0.47	$6.5 \times 10^4$	$3.9 \times 10^{-3}$
$1.8 \times 10^{-1}$	$1.8 \times 10^2$	0.01	0.01	$5.9 \times 10^5$	$1.3 \times 10^{-3}$
	$5.6 \times 10^2$	0.04	0.04	$1.9 \times 10^5$	$2.3 \times 10^{-3}$
	$1.8 \times 10^3$	0.13	0.13	$5.4 \times 10^4$	$4.3 \times 10^{-3}$
	$5.6 \times 10^3$	0.40	0.47	$1.3 \times 10^4$	$8.6 \times 10^{-3}$
$5.6 \times 10^{-1}$	$5.6 \times 10^2$	0.01	0.01	$2.9 \times 10^4$	$5.9 \times 10^{-3}$
	$1.8 \times 10^3$	0.04	0.04	$8.3 \times 10^3$	$1.1 \times 10^{-2}$
	$5.6 \times 10^3$	0.13	0.13	$1.9 \times 10^3$	$2.3 \times 10^{-2}$
	$1.8 \times 10^4$	0.40	0.47	$4.2 \times 10^2$	$4.8 \times 10^{-2}$

Table 1: *The kinematic variables  $x, Q^2, y$ , and  $D$ , along with the number of events expected  $N_{total}$ , and the statistical uncertainty in the measured asymmetry  $\delta A_m$  in the kinematical region assuming an integrated luminosity  $L = 1000 \text{ pb}^{-1}$  and proton and electron beam polarizations  $P_p = P_e = 0.7$ .*

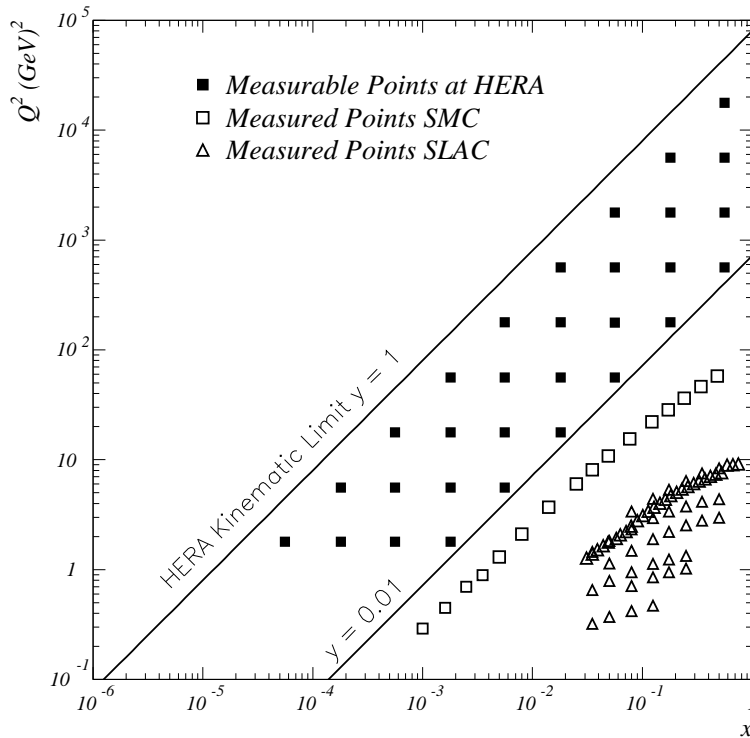


Figure 2: Measurable  $x - Q^2$  region at HERA shown with the presently explored regions by SMC(CERN) and E143(SLAC) experiments, and the kinematic limit of measurability at HERA.

## 2.2 Systematic errors for HERA data

The systematic errors associated with spin dependent asymmetry measurements are of two types: 1) normalization errors and 2) false asymmetries.

The normalization errors include principally uncertainties in the electron polarization  $P_e$  and in the proton polarization  $P_p$ . These lead to a change in the magnitude of the measured asymmetry but in practice by an amount which is small compared to the statistical error, and hence they are important primarily when evaluating the first moment of  $g_1^p(x)$ .

Recently the HERMES collaboration has reported a measurement of  $P_e$  by Compton scattering, which yielded a relative accuracy of 5.5% [11]. It is expected that an improved accuracy will be achieved eventually.

Absolute measurement of the polarization of the high energy (800 GeV) proton beam presents a new challenge and is presently under investigation. Several methods are being considered:

1.  $p - p$  elastic scattering in the Coulomb-nuclear interference region[12],
2.  $p - \bar{p}$  scattering using a stationary polarized proton jet target and comparing the asymmetries  $A_{\text{beam}} = A_{\text{jet}}$ , where  $A_{\text{beam}}$  is the asymmetry in the scattering of the polarized beam from an *unpolarized* jet and  $A_{\text{jet}}$  is the asymmetry measured with an *unpolarized* beam and a polarized jet target with a known polarization  $P_{\text{jet}}$ . Adjusting the jet polarization to obtain the same asymmetry, one obtains the beam polarization  $P_{\text{beam}} = P_{\text{jet}}$  [13].

3. polarized  $e - p$  scattering in which a low energy polarized electron beam collides with the polarized 800 GeV proton beam, with kinematics corresponding to the polarized  $e - p$  elastic scattering measurements at SLAC [14]. The theoretical values for the asymmetry in elastic scattering are given in terms of the polarizations and the measured electric and magnetic form factors of the proton. Hence the measured asymmetry at HERA using a known polarized electron beam would determine  $P_p$ .

We comment briefly on these possible methods. For method 1 the nuclear matrix element may not be known well enough to provide a significant absolute determination of  $P_p$ . Method 2 appears quite attractive because only the invariance principle is needed from theory, and it may be possible to use the stationary polarized target of the HERMES experiment for this measurement. Method 3 is theoretically sound and simple, but may not be attractive experimentally. These methods have still to be fully developed and tested experimentally. It is reasonable to expect that a 5% accuracy will be achieved.

Inclusive  $\pi^+$  or  $\pi^-$  production in collisions of 800 GeV protons with a fixed proton target appears to be a simple method for a relative measurement of the polarization [15].

Methods to measure  $P_p$  are presently considered and studied also for polarized protons at RHIC. The method of measuring  $P_p$  at 1 TeV has been discussed in some detail in a design report entitled “Acceleration of Polarized Protons to 120 GeV and 1 TeV at Fermilab” [16] as well as in the BNL proposal for RHIC SPIN [17].

The other type of systematic error comes from false asymmetries. These arise from variations in counting rate due to time variations in detector efficiencies, beam intensities, or crossing angles between the conditions of spins parallel and antiparallel. In view of the expected small values of the true asymmetries expected in the HERA kinematic region, (Table 1), the false asymmetries must be controlled at the level of  $10^{-4}$ . We note that medium and high energy experiments which have measured parity violation have controlled false asymmetries to less than  $10^{-5}$  to  $10^{-8}$  [18].

False asymmetries can be avoided by frequent reversals of spin orientations. In the HERA collider the electron(positron) spin reversal is difficult and time consuming (several hours) and would lead to changes in beam intensity and beam emittance. Hence asymmetry data must be obtained with a fixed helicity for the electron beam by varying the proton helicity. Both the electron and proton rings are filled with about 200 particle bunches. The proton ring can be filled with bunches of protons with individually predetermined polarizations. Parallel and antiparallel spin data would be obtained at successive beam crossings occurring at time intervals of about 100 ns. Such alternations eliminate many errors in an asymmetry measurement. However, differences in the intensities and the crossing angles at successive proton bunches could still lead to false asymmetries and will have to be minimized.

The most important approach to avoid false asymmetries will be to use a spin rotator to reverse the helicity of all proton bunches at adequately frequent intervals (perhaps once per 8 hours). The design of such rotators has been studied and appears practical without appreciable change in the orbits, or in the magnitude of proton polarization [19]. Studies at the IUCF at 370 MeV have confirmed these conclusions [20]. With such approach the false asymmetries could be controlled to less than  $10^{-4}$ .

### 3 Current status of $g_1(x, Q^2)$

#### 3.1 Perturbative evolution of $g_1(x, Q^2)$

The definition and properties of the polarized structure function  $g_1$  in perturbative QCD closely parallel that of its unpolarized counterpart  $F_2$  (see ref. [21] for a review). The structure function  $g_1$  is related to the polarized quark and gluon distributions through

$$g_1(x, t) = \frac{1}{2}\langle e^2 \rangle \int_x^1 \frac{dy}{y} \left[ C_q^S\left(\frac{x}{y}, \alpha_s(t)\right) \Delta\Sigma(y, t) + 2n_f C_g\left(\frac{x}{y}, \alpha_s(t)\right) \Delta g(y, t) + C_q^{\text{NS}}\left(\frac{x}{y}, \alpha_s(t)\right) \Delta q^{\text{NS}}(y, t) \right], \quad (1)$$

where  $\langle e^2 \rangle = n_f^{-1} \sum_{k=1}^{n_f} e_k^2$ ,  $t = \ln(Q^2/\Lambda^2)$ ,  $\Delta\Sigma$  and  $\Delta q^{\text{NS}}$  are the singlet and non-singlet polarized quark distributions

$$\Delta\Sigma(x, t) = \sum_{i=1}^{n_f} \Delta q_i(x, t), \quad \Delta q^{\text{NS}}(x, t) = \sum_{i=1}^{n_f} (e_i^2/\langle e^2 \rangle - 1) \Delta q_i(x, t),$$

and  $C_q^{S,NS}(\alpha_s(Q^2))$  and  $C_g(\alpha_s(Q^2))$  are the quark and gluon coefficient functions.

The  $x$  and  $Q^2$  dependence of the polarized quark and gluon distributions is given by Altarelli-Parisi equations [22]:

$$\frac{d}{dt} \Delta\Sigma(x, t) = \frac{\alpha_s(t)}{2\pi} \int_x^1 \frac{dy}{y} \left[ P_{qq}^S\left(\frac{x}{y}, \alpha_s(t)\right) \Delta\Sigma(y, t) + 2n_f P_{qg}\left(\frac{x}{y}, \alpha_s(t)\right) \Delta g(y, t) \right], \quad (2)$$

$$\frac{d}{dt} \Delta g(x, t) = \frac{\alpha_s(t)}{2\pi} \int_x^1 \frac{dy}{y} \left[ P_{gq}\left(\frac{x}{y}, \alpha_s(t)\right) \Delta\Sigma(y, t) + P_{gg}\left(\frac{x}{y}, \alpha_s(t)\right) \Delta g(y, t) \right], \quad (3)$$

$$\frac{d}{dt} \Delta q^{\text{NS}}(x, t) = \frac{\alpha_s(t)}{2\pi} \int_x^1 \frac{dy}{y} P_{qq}^{\text{NS}}\left(\frac{x}{y}, \alpha_s(t)\right) \Delta q^{\text{NS}}(y, t), \quad (4)$$

where  $P_{ij}$  are polarized splitting functions.

The full set of coefficient functions [23] and splitting functions [24] has been computed up to next-to-leading order in  $\alpha_s$ . As in any perturbative calculation, at next-to-leading order splitting functions, coefficient functions and parton distributions depend on renormalization and factorization scheme, while of course physical observables, such as  $g_1$  itself, remain scheme-independent up to terms of order  $\alpha_s^2$ . The scheme choice is arbitrary, and in particular parton distributions in different factorization schemes are related to each other by well-defined linear transformations.

The factorization scheme dependence is particularly subtle in the polarized case because of the extra ambiguity related to the definition of the  $\gamma_5$  matrix, i.e. to the way chiral symmetry is broken by the regularization procedure. This is reflected in an ambiguity in the size of the first moment of the gluon coefficient function  $C_g$  (which starts at order  $\alpha_s$ ). Two widely adopted choices [8, 25, 26], both compatible with the choice of  $\overline{\text{MS}}$  renormalization and factorization, correspond to either requiring the first moment of the gluon coefficient function to be  $C_g^1 = 0$ , or imposing that the first moment of the polarized quark distribution be scale independent, which implies  $C_g^1 = -\frac{\alpha_s}{4\pi}$ . The first moment  $\Delta g^1$  of the gluon distribution can be chosen to be the same in the two schemes, whereas the first moments of the quark distribution in the two schemes differ by an amount proportional to  $\alpha_s \Delta g^1$ . Because the evolution equations 2-4 imply that at leading order the first moment of the polarized gluon scales as  $\frac{1}{\alpha_s}$  this scheme dependence persists asymptotically and is potentially large if the first moment of the gluon distribution is large [27].

## 3.2 Current status of polarized parton distributions.

Parton distributions can be extracted from experimental structure function data by parametrizing them at a starting value of  $Q^2$ , evolving this initial condition up to any desired value of  $x$  and  $Q^2$  using Eqs. 2-4, determining  $g_1$  there by means of Eq. 1, and determining the initial parametrization which gives the best fit of  $g_1(x, Q^2)$  to the data [8, 25, 26]. Here we follow the procedure used in refs. [8, 28]: we give the initial conditions at  $Q^2 = 1 \text{ GeV}^2$  in the form

$$\Delta f(x, Q^2) = N(\alpha_f, \beta_f, a_f) \eta_f x^{\alpha_f} (1-x)^{\beta_f} (1+a_f x), \quad (5)$$

where  $N(\alpha, \beta, a)$  is fixed by the normalization condition,  $N(\alpha, \beta, a) \int_0^1 dx x^\alpha (1-x)^\beta (1+ax) = 1$ , and  $\Delta f$  denotes  $\Delta\Sigma$ ,  $\Delta q_{NS}$ , or  $\Delta g$ . With this normalization the parameters  $\eta_g, \eta_{NS}$ , and  $\eta_S$  are respectively the first moments of the gluon, the non-singlet quark and the singlet quark distributions at the starting scale. Evolution is performed within the AB factorization scheme (which has  $C_g^1 = -\frac{\alpha_s}{4\pi}$ ). Further details of the fits and analysis are given in ref. [8, 28].

The results of the NLO fit of Ref. [8] (based on the data of Ref.s [6, 7]) are shown in Fig. 3. Interestingly, the data require the first moment of the gluon distribution to differ significantly from zero:  $\eta_g = 1.52 \pm 0.74$ . This result follows mostly from the observed scaling violations in the intermediate and small  $x$  region. However, the statistical uncertainty on the size of the polarized gluon distribution is still rather large. Moreover, existing data only partially constrain the small  $x$  behaviour of the various parton distributions (values of  $\alpha_S, \alpha_g$ , and  $\alpha_{NS}$ ), and do not allow a precise determination of their asymptotic form for small  $x$ . Such information, besides its intrinsic theoretical interest, is required in order to obtain a precise determination of the moments of  $g_1$  [8, 28]. New data with an extended kinematic coverage in  $x$  and  $Q^2$  provided by HERA could reduce these uncertainties.

Since the publication of ref. [8], new data on the  $Q^2$  dependence of  $g_1$  have been published by the E143 collaboration[29]. The inclusion of these data in the NLO fits<sup>2</sup>, results in values of the fitted parameters (shown in column 2 of Table 2) whose central values are consistent with the previously published ones [8], while errors are reduced of up to 20%. The value of the first moment of the gluon distribution at  $Q^2 = 1 \text{ GeV}^2$  in particular becomes  $\eta_g = 1.30 \pm 0.56$ . In the next two years both SMC (CERN) and E143 (SLAC) plan to present new data on proton and deuteron spin structure functions and using these data as well a more accurate determination of the parameters in the fit can be expected. It can thus be anticipated that eventually the dominant uncertainty in the determination of the first moments of  $g_1$  and the polarized gluon distribution will be due to lack of experimental information in the HERA region.

## 4 The impact of polarized HERA data

### 4.1 The small $x$ behaviour of $g_1$

As shown in Fig. 2, measurements of  $g_1$  at HERA will extend the  $x$  region down to  $x = 5.6 \times 10^{-5}$ . Knowledge of the small  $x$  behaviour of  $g_1$  is obviously necessary in order to compute moments of  $g_1$ , and indeed in the determination of the singlet component of the first moment of  $g_1$  the

---

<sup>2</sup>We have excluded data from ref. [29] corresponding to the beam energy of 29.1 GeV, which duplicate previously published data [7], as well as data with  $Q^2 < 0.95 \text{ GeV}^2$ .



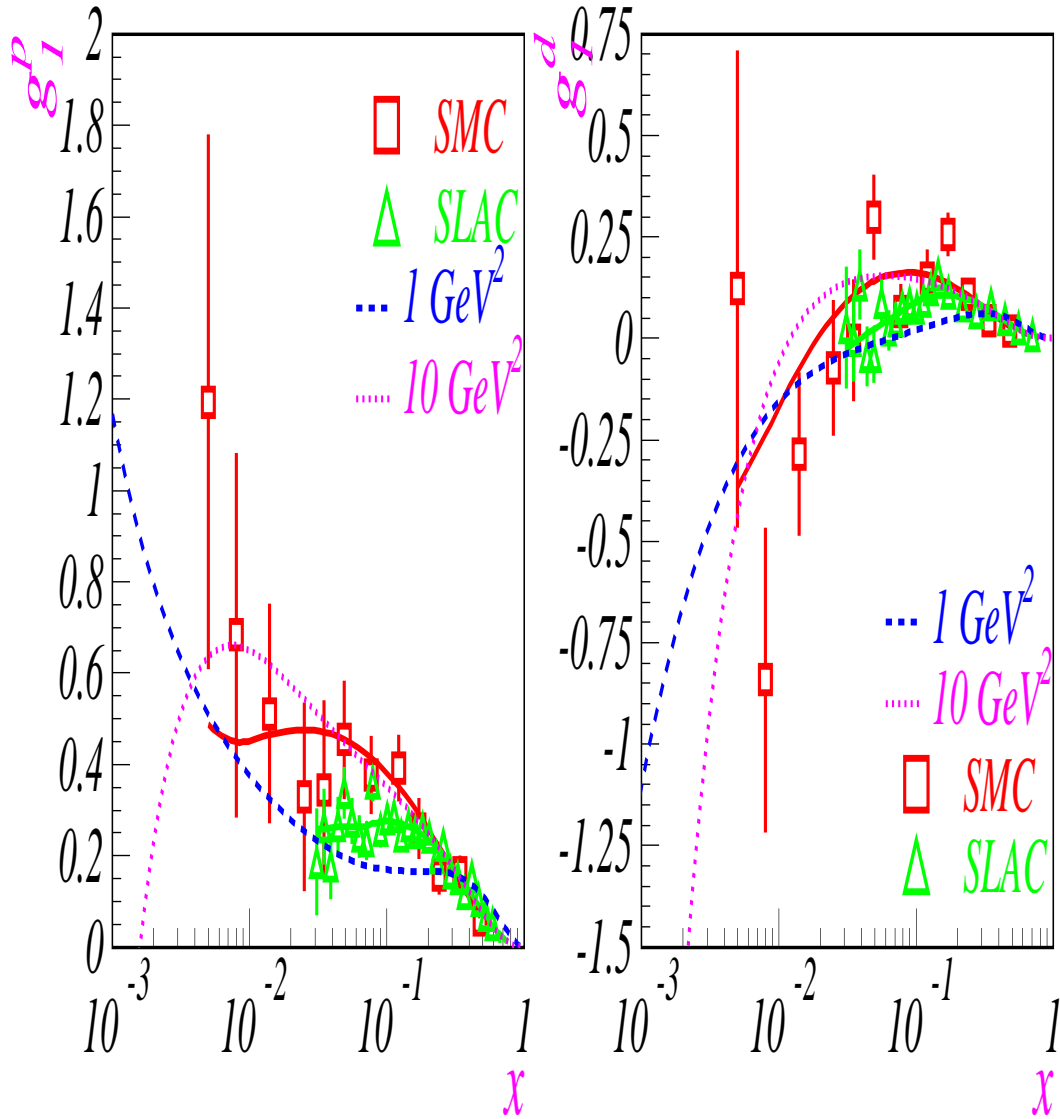


Figure 3: *The NLO fit to proton  $g_1^p$  and deuteron  $g_1^d$  data. The solid lines are fits to data at the measured  $Q^2$  values, and the dashed and the dotted lines are fits evolved to  $Q^2 = 1$  and  $10 \text{ GeV}^2$  respectively.*

uncertainty related to the lack of knowledge of this behaviour is already comparable to the statistical uncertainty [8, 28].

The extrapolation of  $g_1$  from the measured region down to  $x = 0$  is traditionally done by assuming Regge behaviour of the structure function, which implies [30]  $g_1 \sim x^\alpha$  as  $x \rightarrow 0$  with  $0 \leq \alpha \leq 0.5$ , i.e. a valence-like behaviour of  $g_1$ . This behaviour seems to disagree with the data (see Table 2 and Fig. 3) which suggest instead that the magnitude of both the singlet and nonsinglet components of  $g_1$  increase at small  $x$ .

In fact, a valence-like behaviour of  $g_1$  is incompatible with perturbative QCD, which at leading order predicts instead that  $g_1$  should rise in magnitude at least as  $g_1(x, Q^2) \sim \frac{1}{\sqrt{\sigma}} e^{2\gamma\sigma}$ , where  $\sigma \equiv \sqrt{\xi\zeta}$ ,  $\rho \equiv \sqrt{\xi/\zeta}$ ,  $\xi \equiv \ln \frac{x_0}{x}$ ,  $\zeta \equiv \ln \frac{\alpha_s(Q_0^2)}{\alpha_s(Q^2)}$ , and  $Q_0$  and  $x_0$  are reference values of  $x$  and  $Q^2$ . This rise is present both in the singlet and nonsinglet components of  $g_1$ , but with different slopes  $\gamma$ , calculable in perturbative QCD. The sign of this rise depends on the specific form of the quark and gluon distributions, but for most reasonable forms of  $\Delta q$  and  $\Delta g$ , and in particular if  $\Delta g$  at moderately small  $x$  is positive definite, then  $g_1$  will be negative. The onset of this behaviour as  $Q^2$  is raised is clearly shown in Fig. 3. Higher order corrections lead to an even stronger drop: at  $k$ -th perturbative order the rise of  $-g_1$  is enhanced by a factor of  $\alpha_s^k \rho^{2k+1}$ . It has been suggested [31] that these terms to all orders in  $\alpha_s$  may exponentiate, thus leading to a rise of  $g_1$  as a power of  $x$ ; the sign of this rise is still predicted to be negative.

A non-Regge behaviour of the unpolarized structure function  $F_2$  has been observed and accurately measured at HERA, in spectacular agreement with the perturbative QCD prediction [9, 10]. The behaviour correspondingly predicted in the polarized case is even more interesting due to the fact that higher order corrections are stronger, and also the polarized singlet and nonsinglet quark and gluon distributions all display qualitatively the same behaviour, whereas in the unpolarized case only the gluon dominates at small  $x$ .

An experimental measurement of the small  $x$  behaviour of  $g_1$  would thus lead to significant insight on the structure of QCD both within and beyond perturbation theory. In Fig. 4 we show the expected accuracy of the determination of  $g_1$  at HERA within the maximal extent of variation in the small  $x$  behaviour compatible with the requirement of integrability of  $g_1$  (which implies that at small  $x$   $g_1$  can rise at most as  $1/(x \ln^\alpha x)$  with  $\alpha > 1$ ).

The full coverage of HERA experiments is shown in Figs. 5, 6, 7, and 8, where projected data with their estimated errors are given on the basis of the NLO fit of Table 2. The errors are estimated assuming integrated luminosities  $L = 1000 \text{ pb}^{-1}$  and beam polarizations  $P_p = P_e = 0.7$ . In Fig. 5  $g_1$  at the starting scale  $Q^2 = 1 \text{ GeV}^2$  is shown using the best fit values of the parameters. This is then evolved up with different choices for the normalization of the polarized gluon distribution, to give a feeling for the possible range of variation. In particular, we consider two cases: a) the first moment of the gluon distributions is fixed to be 0 at  $Q^2 = 1 \text{ GeV}^2$  (minimal gluon: dashed lines in Fig.6) and b) the first moment of the singlet quark density was fixed to  $\eta_q = a_8$  at the same reference scale (maximal gluon: dotted lines in Fig.6). Even though the current best fit value of  $\eta_g$  (Table 2) is very close to the maximal case, the minimal gluon is at present only excluded at  $2 \sigma$  level. Of course yet wider deviations from these fits are foreseeable since the small  $x$  behaviour of the current best fit is only very loosely constrained due to the lack of direct experimental information at small  $x$ ; also, as discussed above, higher order corrections beyond NLO may turn out to be important at very small  $x$ .

In Fig. 6 we show the statistical errors for each measurable data point in the complete  $x - Q^2$  grid indicated in Fig. 2 and in Table 1. The bold solid lines are the predictions of

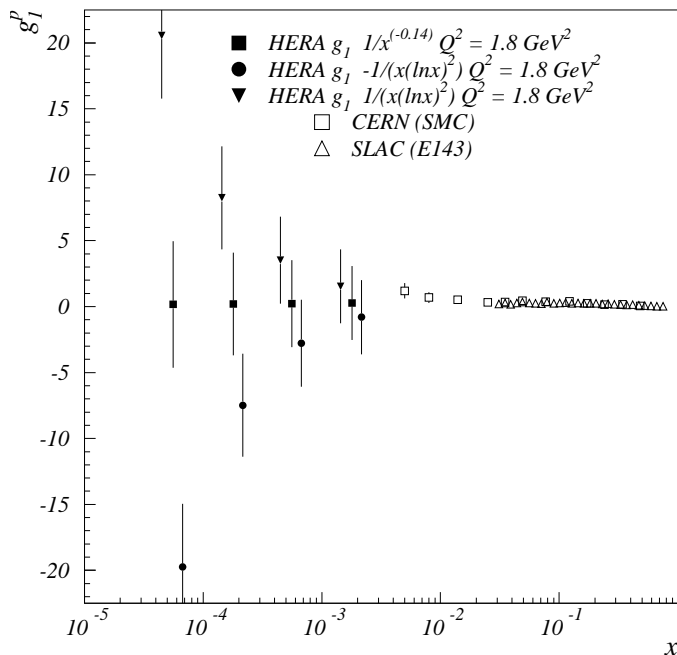


Figure 4: The structure function  $g_1^p$  measurable at HERA for  $Q^2 = 1.8 \text{ GeV}^2$  with integrated luminosity  $L = 1000 \text{ pb}^{-1}$  are shown. The SMC and E143 measurements are shown for comparison. Starting from the measured values of  $g_1^p$  by SMC, the measurable values for HERA at low- $x$  are shown in two extreme cases: valence-like behaviour  $g_1(x) \sim x^{-\alpha}$  with  $\alpha = 0.14$  or strong powerlike positive or negative rises  $g_1(x) \sim \pm 1/(x \cdot (\ln x)^2)$

$g_1$  values in the HERA kinematic range using the best fit values of the NLO parameters for the presently published data [6, 7]. In Fig. 7 the projected values of  $g_1$  obtained from the NLO fit to the data are calculated for the lowest  $Q^2$  data point reached at that  $x$  bin, which in turn has the lowest statistical error. The  $Q^2$  values are indicated in the figure. The measured asymmetries  $A_m$  and the corresponding statistical errors on the projected measurements at HERA at different  $Q^2$  are shown in Fig. 8.

## 4.2 The determination of the gluon distribution

The measurement of scaling violations in inclusive structure functions provides a theoretically clean determination of the polarized gluon distribution. Because the gluon distribution is only determined by the scale dependence of the moments of  $g_1$  a reasonably wide kinematic coverage is required in order to achieve such a determination with satisfactory accuracy: in particular, since the gluon distribution is peaked at small  $x$ , data in this region for several values of  $Q^2$  such as those obtainable at HERA would substantially improve the determination of  $\Delta g(x, Q^2)$ .

To assess the impact of these data we have repeated the fit described in sect. 3.2 with the addition of the projected HERA data discussed in sect. 2.1. The values of the best-fit parameters of course do not change, but using the estimated errors from acceptance considerations on measurable  $g_1$ , we get an estimate of the extent of reduction in the measured uncertainties of various parameters. In column 3 of Table 2 we show the results of a fits with HERA data for integrated luminosity  $L = 1000 \text{ pb}^{-1}$  and in column 4 we show the results for  $L = 200 \text{ pb}^{-1}$ .

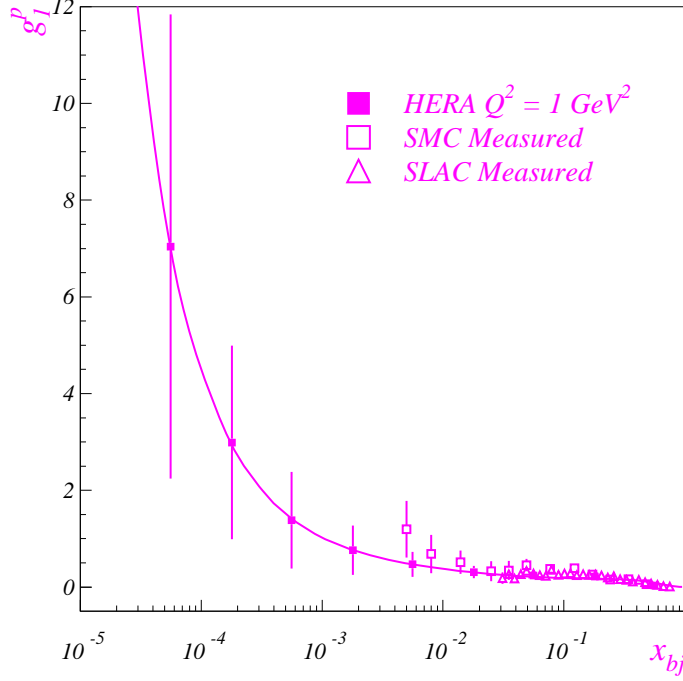


Figure 5: The starting parametrization of  $g_1^p$  at  $Q^2 = 1 \text{ GeV}^2$  which gives best-fit to present-day data is shown in the  $x$  range covered at HERA. Statistical errors on  $g_1$  after combining all measurements for each  $x$  are shown for an integrated luminosity  $L = 1000 \text{ pb}^{-1}$ .

Parameter	Published data	HERA $L = 1000 \text{ pb}^{-1}$	HERA $L = 200 \text{ pb}^{-1}$
$\eta_g$	$1.30 \pm 0.56$	$1.29 \pm 0.22$	$1.29 \pm 0.28$
$\eta_q$	$0.45 \pm 0.05$	$0.45 \pm 0.04$	$0.45 \pm 0.05$
$\eta_{NS}$	Fixed	Fixed	Fixed
$\alpha_g$	$-0.64 \pm 0.26$	$-0.64 \pm 0.11$	$-0.64 \pm 0.16$
$\alpha_q$	$0.42 \pm 0.35$	$0.42 \pm 0.26$	$0.42 \pm 0.30$
$\alpha_{NS}$	$-0.73 \pm 0.14$	$-0.73 \pm 0.10$	$-0.73 \pm 0.12$
$\beta_g$	4.0 (fixed)	4.0 (fixed)	4.0 (fixed)
$\beta_q$	$3.53 \pm 0.87$	$3.50 \pm 0.81$	$3.50 \pm 1.13$
$\beta_{NS}$	$2.18 \pm 0.28$	$2.10 \pm 0.27$	$2.10 \pm 0.14$
$a_q = a_g$	$1.2 \pm 2.8$	$1.2 \pm 2.5$	$1.2 \pm 2.10$
$a_{NS}$	$19.5 \pm 20.4$	$19.5 \pm 14.0$	$19.5 \pm 16.4$

Table 2: Results of NLO fits: Column 2: fit to all available published data [6, 7, 29]; Column 3: estimated results including data at HERA with integrated luminosity  $L = 1000 \text{ pb}^{-1}$ ; Column 4: estimated results using data at HERA with  $L = 200 \text{ pb}^{-1}$ . The parameter  $\eta_{NS}$  is fixed by the octet hyperon  $\beta$  decay constant.

Note in particular the sizable improvement in the determination of the first moment of  $\Delta g$ , which is of greatest theoretical interest due to its role in the understanding of the proton spin structure [5]: from  $\delta(\Delta g^1) = \pm 0.56$  (the present value) to  $\pm 0.22$  or  $\pm 0.28$  depending on the luminosity available at HERA.

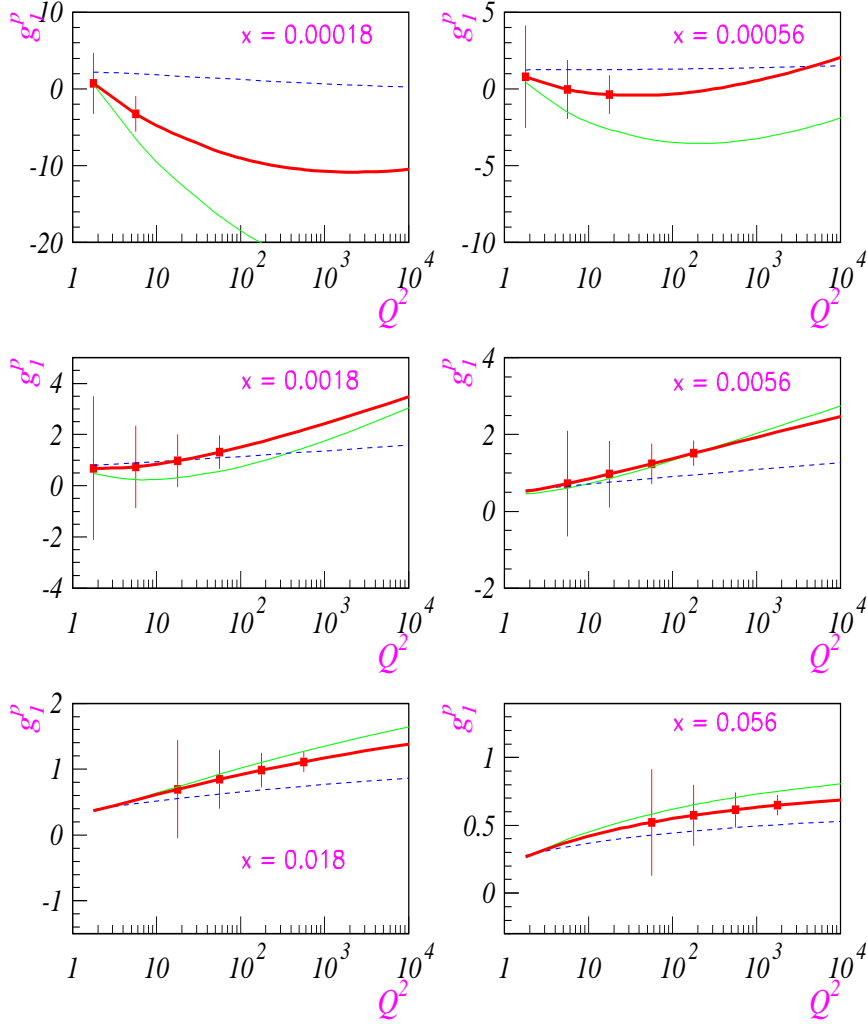


Figure 6: Predicted values for  $g_p^1$  from NLO fits together with estimated statistical uncertainties for a future polarized DIS experiment with an integrated luminosity  $L=1000 \text{ pb}^{-1}$ . The solid bold lines are predictions based on fits to SMC and SLAC data extended in to the HERA kinematic range while the dotted and dashed lines are the maximal and minimal gluon predictions (see text).

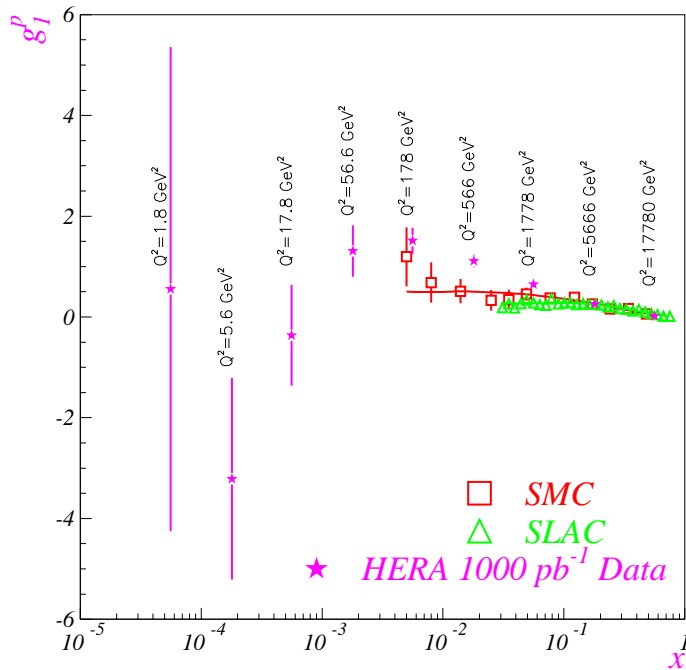


Figure 7: The structure function  $g_1^p$  measurable at HERA shown in comparison to the SMC/E143 measurements. The values of  $g_1^p(x, Q^2)$  for each measurable HERA point are taken from the NLO fit and evolved to the  $Q^2$  value indicated in the figure. Statistical errors on  $g_1(x)$  averaged over all  $Q^2$  for measurements at HERA with integrated luminosity  $L = 1000 \text{ pb}^{-1}$  are shown for each  $x$ .

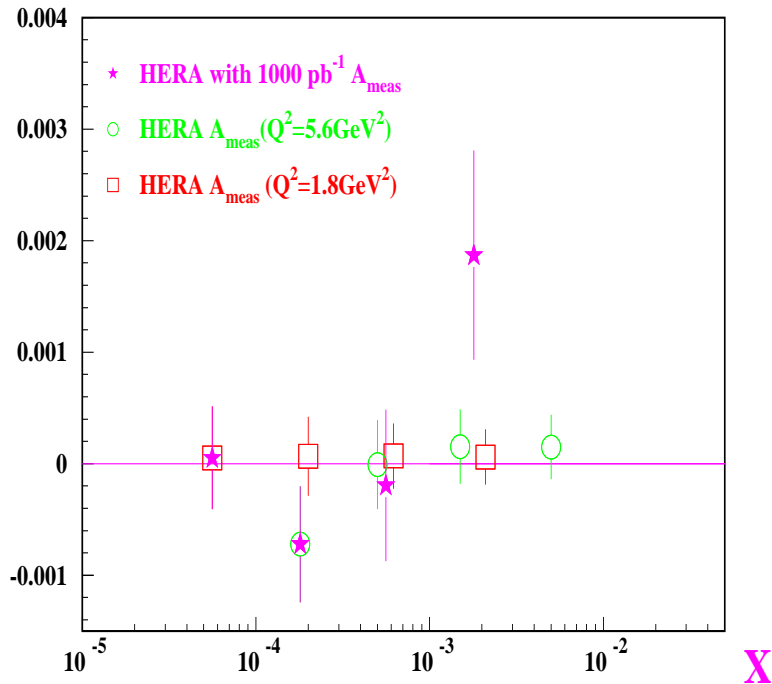


Figure 8: The measured asymmetry  $A_m$  for different  $Q^2$  at HERA for the projected data points shown in previous figures.

## 5 Conclusions

Inclusive DIS measurements at HERA with high integrated luminosity with high energy polarized electrons and polarized protons would yield significant and unique new information on  $g_1^p(x, Q^2)$  over a much extended range in  $x$  and  $Q^2$ . For such measurements the false asymmetries should be considerably smaller than the true asymmetries to be measured, and normalization systematic errors should be controlled to be less than 10%. Statistical errors on the points will dominate.

There is a strong and broad current interest in the spin structure of the nucleon. Proposals have been made and experiments are planned to study this problem at several accelerator facilities. These include COMPASS at CERN, a possible experiment at SLAC, and RHIC SPIN at BNL. A principal goal of all of these proposed experiments is to measure the polarized gluon content in the nucleon from a study of semi-inclusive processes. Another experiment involving a semi-inclusive process is discussed in this volume where the determination of  $\Delta g$  from a study of dijets from polarized e-p collisions at HERA is described. A measurement of  $\Delta g$  from inclusive process has the advantage of being theoretically clean, but requires a wide kinematic coverage in  $x$  and  $Q^2$ , and could thus only be performed at HERA.

The inclusive measurements with HERA discussed in this chapter will also provide unique information on the behaviour  $g_1^p(x, Q^2)$  over an unexplored kinematic range, which is of great theoretical interest.

The fact that HERA is an operating facility with a plan for substantial increase in luminosity and with two major operating detectors, as well as a polarized electron beam, means that

only the high energy polarized proton beam needs to be developed. The efforts to achieve that seem well justified and data from such experiments at HERA would provide unique and complementary information to that from other presently proposed experiments.

## Appendix: Kinematics of polarized DIS at HERA

The polarized structure function  $g_1^p$  of the proton is related to the virtual photon asymmetry  $A_1^p$  by the relation [32],

$$g_1 = \frac{F_2}{2x(1+R)} A_1 \quad (6)$$

in terms of the unpolarized structure function  $F_2$  and the ratio of longitudinal to transverse photoabsorption cross sections  $R$ .<sup>3</sup> The measured longitudinal asymmetry  $A_m$  is related to  $A_1$  by,

$$A_m = \frac{N^{\uparrow\uparrow} - N^{\uparrow\downarrow}}{N^{\uparrow\uparrow} + N^{\uparrow\downarrow}} = P_p P_e D A_1 \quad (7)$$

where  $P_p(P_e)$  is the proton (electron) polarization, and  $D$  is the depolarization factor. The arrows indicate the relative direction of the spins of the electrons and protons.  $D$  is calculable from QED and is given by

$$D = \frac{y(2-y)}{y^2 + 2(1-y)(1+R)}, \quad (8)$$

where

$$y = \frac{Q^2}{xs} \quad (9)$$

and  $s$  is the Mandelstam invariant of the electron-proton collision. The dependence of  $D$  on  $y$  is shown in Fig. 9. The statistical uncertainty  $\delta A_m$  in the measurement of  $A_m$  is given by,

$$\delta A_m = \frac{1}{\sqrt{N^{\uparrow\uparrow} + N^{\uparrow\downarrow}}} = \frac{1}{\sqrt{N_{total}}} \quad (10)$$

where  $N^{\uparrow\uparrow}$  ( $N^{\uparrow\downarrow}$ ) represent the number of DIS events observed with parallel (anti parallel) proton and electron polarizations, respectively. The sum in the denominator is then the square root of the total number of events observed in the experiment at selected  $x - Q^2$  bins.

We estimate the yield and the associated statistical error to be observed in a future HERA experiment. The cross section for DIS is given by

$$\frac{d^2\sigma}{dx dQ^2} = \frac{4\pi\alpha^2}{xQ^4} \left[ 1 - y + \frac{y^2}{2(1+R)} \right] F_2 \quad (11)$$

The depolarization factor  $D$  for each of the bins was calculated and used to estimate the statistical uncertainty in the measurement of  $g_1^p$  from Eqs. 8 and 10.

**Acknowledgements:** We thank G. Altarelli and P. Schuler for interesting discussions and helpful comments.

---

<sup>3</sup>This result holds at leading twist.



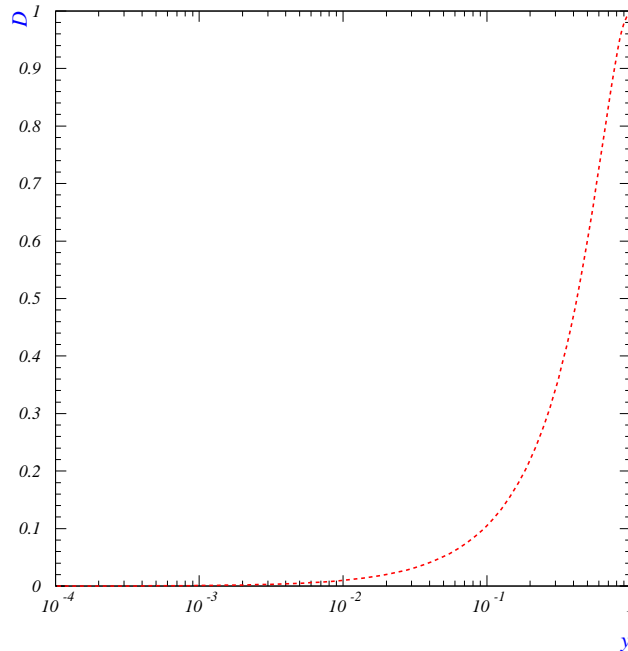


Figure 9: *The dependence of depolarization factor  $D$  on  $y$ .*

## References

- [1] R. Hofstadter, Rev. Mod. Phys. **28** (1956) 214.
- [2] J. Friedman et al., Ann. Rev. Nucl. Science **22**, (1972), 203.
- [3] SLAC E80, M. J. Alguard et al., Phys. Rev. Lett. **37** (1976) 1261; *ibid* **41** (1978) 70; SLAC E130, G. Baum et al., Phys. Rev. Lett. **51** (1983) 1135.
- [4] EMC, J. Ashman et al., Nucl. Phys. **B328** (1989) 1.
- [5] See e.g. G. Altarelli and G. Ridolfi, Nucl. Phys. B Proc. Suppl. **39B** (1995) 106; R. D. Ball, [hep-ph/9511330](#), in the proceedings of the Erice school on nucleon spin structure; S. Forte, [hep-ph/9511345](#), in the proceedings of the 7th Rencontres de Blois.
- [6] SMC, B. Adeva et al., Phys. Lett. **B302** (1993) 533; SMC, D. Adams et al., Phys. Lett. **B329** (1994) 399; SMC, D. Adams et al., Phys. Lett. **B357** (1995) 248.
- [7] E-143, K. Abe et al., Phys. Rev. Lett. **74** (1995) 346; E-143, K. Abe et al., Phys. Rev. Lett **75** (1995) 25.
- [8] R. D. Ball, S. Forte and G. Ridolfi, Phys. Lett. **B378** (1996) 255.
- [9] A. De Roeck, lectures at the 1994 Cargèse school, preprint DESY-95-025.
- [10] R.D. Ball and A. De Roeck, in “DIS96” (World Scientific, 1996), [hep-ph/9609309](#)
- [11] HERMES Collaboration, in “DIS96” (World Scientific, 1996).

- [12] N. Akchurin et al., Phys. Rev. **D48** (1993) 3026.
- [13] L. Wolfenstein, Ann. Rev. Nuclear Science **6** (1956) 43.
- [14] M. J. Alguard et al., Phys. Rev. Lett. **37** (1976) 1258.
- [15] D. Adams et al., Phys. Lett. **B246** (1991) 14.
- [16] “Acceleration of Polarized Protons to 120 GeV and 1 TeV at Fermilab”, Michigan preprint HE 95-09, (1995).
- [17] M. Beddo et al., Proposal for spin physics at RHIC (1993)
- [18] C. Y. Prescott et al., Phys. Lett. **B77** (1978) 347; Phys. Lett. **B84** (1979) 524.  
V. Yuan et al., Phys. Rev. Lett. **57** (1986) 320 (and references therein);  
P. A. Souder et al., Phys. Rev. Lett. **65** (1990) 694.
- [19] T. Roser, Nucl. Instr. Meth. **A342** (1994) 343.
- [20] R. A. Phelps et al., Phys. Rev. Lett. **72** (1994) 1479.
- [21] G. Altarelli, Phys. Rep. **81** (1982) 1.
- [22] G. Altarelli and G. Parisi Nucl. Phys. **B126** (1977) 298.
- [23] J. Kodaira et al., Phys. Rev. **D20** (1979) 627.
- [24] R. Mertig and W.L. van Neerven, Z. Phys. **C70** (1996) 637;  
W. Vogelsang, preprint RAL-TR-96-020, hep-ph/9603366 (1996).
- [25] T. Gehrmann and W. J. Stirling, Z. Phys. **C65** (1995) 461; Phys. Rev. **D53** (1996) 6100.
- [26] M. Glück, E. Reya, M. Stratmann and W. Vogelsang, Phys. Rev. **D53** (1996) 4775 .
- [27] G. Altarelli and G. G. Ross, Phys. Lett. **B212** (1988) 391;
- [28] R. D. Ball, S. Forte and G. Ridolfi, Nucl. Phys. **B444** (1995) 287.
- [29] E-143, K. Abe et al., Phys. Lett. **B364** (1995) 61
- [30] R. L. Heimann, Nucl. Phys. **B64** (1973) 429.
- [31] R. Kirschner and L. Lipatov, Nucl. Phys. **B213** (1983) 122;  
J. Bartels, B. I. Ermolaev and M. G. Ryskin, Z. Phys. **C70** (1996) 273; preprint DESY-96-025, hep-ph/9603204
- [32] T. Pussieux and R. Windmolders, preprint DAPNIA-SPHN-95-10, in “Internal Spin Structure of the Nucleon”, V. W. Hughes and C. Cavata, ed.s (World Scientific, Singapore, 1995).